THE TEMPERATURE DEPENDENCE OF THE FERROMAGNETIC RESONANCE LINE WIDTH IN ELECTROPLATED COBALT

Thesis for the Degree of M. S.

MICHIGAN STATE COLLEGE

David Lyman Kingston

1955

This is to certify that the

thesis entitled

The Temperature Dependence of the Ferromagnetic Resonance Line Width in Cobalt

presented by

David Lyman Kingston

has been accepted towards fulfillment of the requirements for

M.S. degree in Physics

R. D. Spence
Major professor

Date May 1 1955

THE TEMPERATURE DEPENDENCE OF THE FERROMAGNETIC RESONANCE LINE WIDTH IN ELECTROPLATED COBALT

by

David Lyman Kingston

A THESIS

Submitted to the School of Graduate Studies of Michigan
State College of Agriculture and Applied Science
in partial fulfillment of the requirements
for the degree of
MASTER OF SCIENCE

Department of Physics

1955

ACKNOWLEDGEMENT

The author wishes to extend his deepest gratitude to Dr. Robert D. Spence who directed this research. His advice, helpful suggestions, and continued interest made the work very enjoyable.

The author also wishes to thank Walter G. Mayer who worked side by side with him for many months.

David L. Kingston

THE TEMPERATURE DEPENDENCE OF THE
FERROMAGNETIC RESONANCE LINE
WIDTH IN ELECTROPLATED COBALT

by

David Lyman Kingston

AN ABSTRACT

Submitted to the School of Graduate Studies of Michigan
State College of Agriculture and Applied Science
in partial fulfillment of the requirements
for the degree of

MASTER OF SCIENCE

Department of Physics
1955

Approved R. D. Spence

David L. Kingston
Thesis Abstract

This thesis reports a study of the temperature dependence of the ferromagnetic resonance line width in electroplated cobalt. At a frequency of 9300 megacycles per seconds, the resonance was found at fields between 400 and 500 gauss, depending on the temperature. The resonance line width in electroplated cobalt is much broader than that found in electroplated nickel and considerably broader than that found in electroplated iron. The line width may be expressed in terms of a reciprocal relaxation time, $1/T_2$. The value of $1/T_2$ is 31 x 10^9 seconds^{-1} at room temperature, decreases to 17 x 10^9 seconds^{-1} at 300 degrees centigrade and remains nearly constant up to 600 degrees centigrade which was the highest temperature at which data were taken. This is to be constrasted with the behavior of electroplated nickel and for electroplated iron. For nickel, $1/T_2$ is 3.1 x 10^9 seconds^{-1} at room temperature and remains fairly constant up to 250 degrees centigrade. At this point it raises very sharply and reaches a value of 5.9 x 10^9 seconds^{-1} at 370 degrees centigrade which is the Curie temperature for nickel. For electroplated iron, $1/T_2$, at room temperature, is 15 x 10^9 seconds^{-1}. It decreases nearly linearly to 7 x 10^9 seconds^{-1} at 600 degrees centigrade.

TABLE OF CONTENTS

LIST OF FIGURES

THE TEMPERATURE DEPENDENCE OF THE FERROMAGNETIC RESONANCE LINE WIDTH IN ELECTROPLATED COBALT

I. INTRODUCTION

Ferromagnetic resonance was discovered by Griffiths[1] in 1946. In his experiment a thin film of ferromagnetic material was placed on one end of a cylindrical microwave resonant cavity. An external magnetic field was applied parallel to the surface of the film. With a constant microwave magnetic field of fixed frequency parallel to the film, but perpendicular to the applied field, it was found that a maximum power absorption occured for a particular value of the external field.

In 1948 Kip and Arnold[2] investigated the ferromagnetic resonance in an iron single crystal as a function of the orientation of the crystal in the applied field. The temperature dependence of the width was first examined by Bloembergen[3] who worked with polycrystalline nickel and supermalloy. His work on the temperature dependence of the line width was extended by Healy[4] who studied ferromagnetic resonance of nickel ferrite as a function of temperature. In 1953 Spence[5] and Cowen[6] examined the temperature dependence of the resonance line width in single crystals of iron and nickel, and electroplated iron and nickel.

A ferromagnetic may be visualized as consisting of a great number of electron spin magnetic moments coupled together by exchange forces to give a resultant magnetic moment. If the applied magnetic field and the r-f field have the correct magnitude and orientation, the ferromagnetic will absorb energy from the r-f field. Quantum mechanically the applied magnetic field splits the degenerate energy levels into a set of Zeeman levels designated by the magnetic quantum numbers m_s. If the selection rule $\Delta m_s = \pm 1$ is satisfied, the r-f field can induce transitions between these levels. Since the most populated level is the lowest energy level the result is an absorption of energy from the r-f field. The absorption continues because the spins give up energy to the crystalline lattice tending to maintain an excess of electrons in the lower state.

At the present time it appears that a satisfactory theoretical explanation of the temperature dependence of the line width has not been given. Bloembergen presented a means of representing the line width by using spin-spin relaxation times and spin-lattice relaxation times. Kittel and Abrahams[7] calculated the temperature dependence of the spin-lattice relaxation. No calculation of the dependence of spin-spin relaxation times have been made. It is a common belief that the spin-spin terms make the major contribution to the line width. Kittel and Abrahams[8] have suggested that at temperatures below one-half the Curie temperature the spin-spin terms predominate, and above one-half the Curie temperature the spin-lattice terms predominate.

II. THEORY

A. FERROMAGNETIC RESONANCE ABSORPTION IN AN ISOTROPIC MEDIUM

A thin sheet of ferromagnetic material, lying in the xy plane, is subjected to a static magnetic field in the z direction and a r-f field in the x direction. The magnetization will consist of a large constant component, M_z and a varying M_x and M_y. The magnetization $\bar{M}$ and the total angular momentum $\bar{J}$ are related by

$$\bar{M} = \gamma \bar{J} \quad , \tag{1}$$

where γ, the magneto-mechanical ratio is

$$\gamma = \frac{ge}{4\pi mc} \quad ,$$

g is the spectroscopic splitting factor, e is the charge of the electron, m is the mass of electron, c is the velocity of light. The classical equations of motion are,

$$\frac{dM_{xy}}{dt} = \gamma \left[\bar{M} \times \bar{H}_{eff} \right]_{xy} - \frac{M_{xy}}{T_2} \quad , \tag{2a}$$

$$\frac{dM_z}{dt} = \gamma \left[\bar{M} \times \bar{H}_{eff} \right]_z - \frac{M_z - M_0}{T_1} \quad . \tag{2b}$$

In the case of an isotropic ferromagnetic material $\bar{M} \times \bar{H}_{eff}$ is the total torque. $\bar{H}_{eff}$ is the effective field inside the material, and is given by

$$\bar{H}_{eff} = \bar{H}_{ext} - N_{xyz}\bar{M} + \bar{H}_{anis} + a\nabla^2\bar{M} , \tag{3}$$

where N_{xyz} is the demagnetization factor. The third term on the right of equation (3) is due to ferromagnetic anisotropy. Since, in this case, the medium is isotropic (see appendix) this term will be dropped. The last term on the right is due to exchange interactions. The exchange effects[9] will be small for pure metals such as cobalt in the temperature range in question. Since this term will have little effect on the effective field, it will be dropped.

The damping terms in equations (2) involve T_1 and T_2. T_1 is the spin-lattice relaxation time, and T_2 is the relaxation time for all effects disturbing the spin system from within. T_1 and T_2 may depend on the frequency of the applied field and on the temperature. In general T_1 and T_2 are not equal.

Following Bloembergen[3] we obtain expressions for the ferromagnetic frequency permeability and resonant frequency. A solution of equations (2) can be obtained by letting $M_{xy} = M_{xy}e^{i\omega t}$. Combining equations (2), (3) and

$$H_x^{ext} = H_1 e^{i\omega t} , \quad H_y^{ext} = 0, \quad H_z^{ext} = H_0 , \tag{4}$$

we get expressions for M_x, M_y, and M_z. In these calculations terms involving products such as M_xM_y, which are small (see figure 1) are dropped. Letting $M_z = M_0$, the last term of

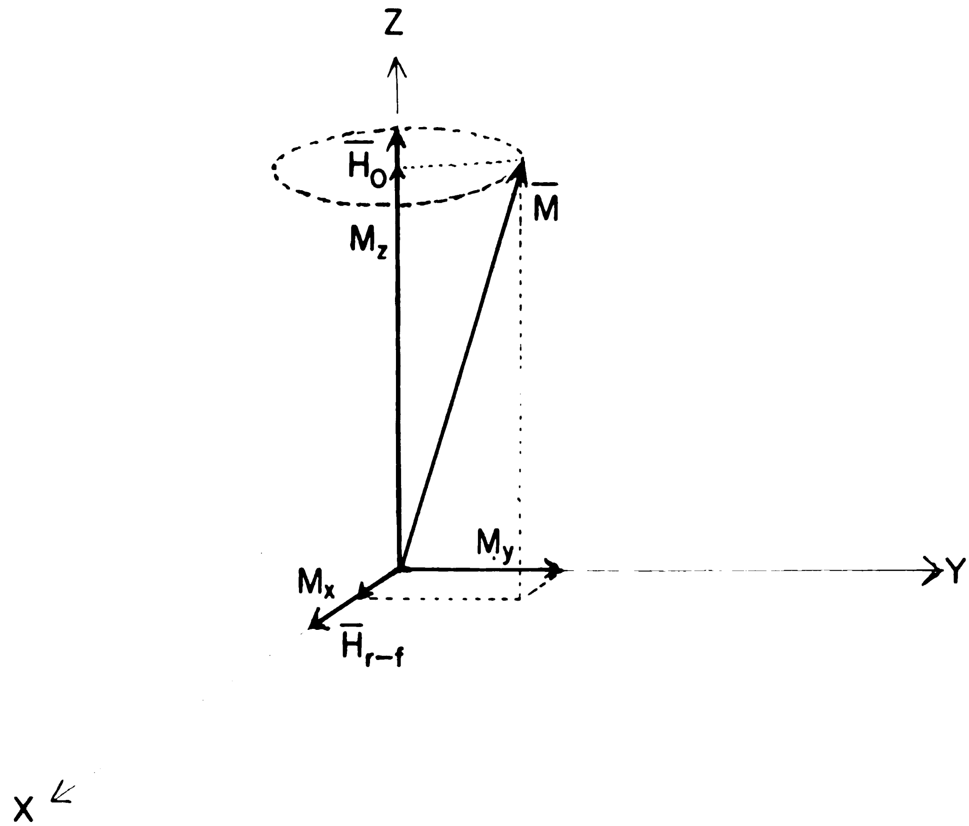

FIGURE I MOTION OF THE MAGNETIZATION VECTOR IN FERROMAGNETIC RESONANCE equation (2b) becomes zero. Hence T_1 drops out of the final equations. Using the relation for the susceptibility,

$$\mu - 1 = \mu_1 - 1 - i\mu_2 = \frac{4\pi M_x}{H_1} \quad , \tag{5}$$

where H_1 is the r-f magnetic field, we get

$$\mu_1 = \frac{4\pi\gamma^2 M_0 \left[H_0 + (N_y - N_z)M_0\right](\omega_0^2 - \omega^2)}{(\omega_0^2 - \omega^2)^2 + 4\omega^2/T_2^2} + 1 \; , \tag{6}$$

$$\mu_2 = \frac{4\pi\gamma^2 M_0 \left[H_0 + (N_y - N_z)M_0\right] \, 2\omega/T_2}{(\omega_0^2 - \omega^2) + 4\omega^2/T_2^2} \quad , \tag{7}$$

where ω_0^2 , the resonant frequency is

$$\omega_0^2 = \gamma^2 \left[H_0 + (N_x - N_z)M_0\right]\left[H_0 + (N_y - N_z)M_0\right] + \frac{1}{T_2} \; . \tag{8}$$

T_2 is the quantity to be evaluated in this experiment.

B. THEORY OF THE USE OF THE RESONANT CAVITY

A microwave resonant cavity is a dielectric filled region completely surrounded by conduction walls, except for an iris which couples the cavity to the rest of the microwave system. The boundary conditions are satisfied by particular configurations and frequencies of electromagnetic field solutions. These normal modes correspond to the resonant frequencies of the cavity. In this experiment we are interested only in those which have linear dimensions of the cavity of the order of the wave length in the wave guide.

For convenience, the cavity may be represented by an equivalent circuit made up of lumped elements. The cavity and coupling iris may be replaced by parallel resonant circuit which is coupled to the transmission line by a transformer (see figure 2)

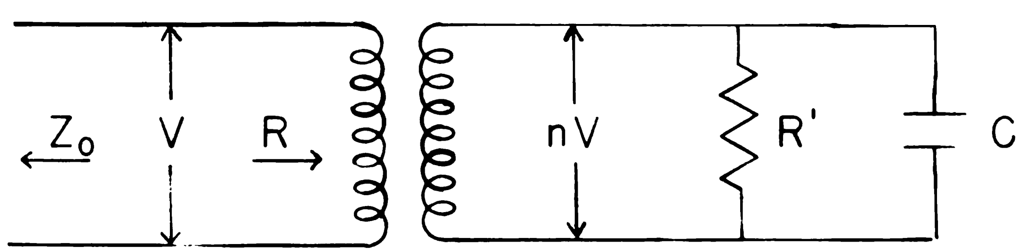

FIGURE 2. EQUIVALENT CIRCUIT OF RESONANT CAVITY

It is assumed that the transmission line is terminated by its characteristic impedance Z_o and the line sees an effective resistance R. The turns ratio of the transformer is n. It is assumed that no energy is lost in the transformer.

With the cavity at resonance, conservation of energy gives

$$\frac{V^2}{R} = \frac{n^2 V^2}{R'} \quad . \tag{9}$$

hence

$$R' = n^2 R \quad ,$$

and (10)

$$Z_o' = n^2 Z_o \quad .$$

The absorbed power is then

$$P_a = \frac{V^2}{R} = \frac{(V_i + V_r)^2}{R} = \frac{V_i^2(1 + \Gamma^2)}{R} \quad , \tag{11}$$

where Γ, the voltage reflection coefficient, is

$$\Gamma = \frac{V_r}{V_i} \quad . \tag{12}$$

At cavity resonance

$$\Gamma = \frac{R - Z_o}{R + Z_o} \quad , \tag{13}$$

and

$$\frac{Z_o}{R} = \frac{1 - \Gamma}{1 + \Gamma} \quad , \tag{14}$$

$$P_a = \frac{V_i^2}{R}(1+\Gamma^2) = \frac{V_i^2}{Z_o}(1-\Gamma^2),\ P_i = \frac{V_i^2}{Z_o},\ P_r = \frac{V_i^2}{Z_o}\Gamma^2, \tag{15}$$

where P_i and P_r are the incident power and the reflected power. They are related to the absorbed power by

$$P_a = P_i - P_r \ . \tag{16}$$

At resonance, the reflection coefficient Γ is real and may be positive or negative since R and Z_o are real. 1/n is a measure of the coupling between the guide and the cavity. In this experiment all the data was taken with an undercoupled cavity. Therefore only the case of the undercoupled cavity will be considered.

For the undercoupled case, 1/n is small compared to Z_o/R', Γ is negative and V_r is negative. Thus

$$\begin{aligned} V_{max} &= V_i - V_r \ , \\ V_{min} &= V_i + V_r \ . \end{aligned} \tag{17}$$

The voltage standing wave ratio is

$$\rho = \frac{V_{max}}{V_{min}} = \frac{V_i - V_r}{V_i + V_r} = \frac{1-\Gamma}{1+\Gamma} = \frac{Z_o}{R} \ . \tag{18}$$

The Q of the cavity will now be defined and related to quantities which can be measured, namely p, $|\Gamma|$, P_r. The total Q is

$$Q = 2\pi \frac{\text{energy stored in cavity}}{\text{total energy lost per period}} \tag{19}$$

The total losses of the cavity are made up of the losses of the unloaded cavity and the external losses. These losses are proportional to the reciprocals of the total Q_t, unloaded Q_u and the external Q_e, respectively.

$$\frac{1}{Q_t} = \frac{1}{Q_u} + \frac{1}{Q_e} \quad . \tag{20}$$

The unloaded Q_u is made up of all of the losses in the cavity proper, Q_c, the losses in the copper walls of the cavity and Q_{fer}, losses in the ferromagnetic sample. The external Q_e is the energy lost by the cavity to the guide.

$$\frac{1}{Q_u} = \frac{1}{Q_c} + \frac{1}{Q_{fer}} \tag{21}$$

The Q_{fer}, is due to the magnetic losses in the sample, and losses due to eddy current and dielectric losses. However, the magnetic losses in the sample are predominate.

The fundamental quantity measured in a ferromagnetic resonance experiment is the ratio of the external Q_e to the unloaded Q_u. This is defined as

$$\frac{Q_e}{Q_u} = \rho = \frac{1+\Gamma}{1-\Gamma} \quad , \tag{22}$$

$$\frac{Q_e}{Q_u} = Q_e \frac{\left(\frac{\rho}{\delta\omega}\iint H^2 d\sigma\right)_{sample} + \left(\frac{\rho}{\delta_1\omega}\iint H^2 d\sigma\right)_{\text{walls of cavity}}}{\left(\iiint H^2 d\tau\right)_{\text{vol. of cavity}}} \quad . \tag{23}$$

where

$$\delta = \sqrt{\frac{\rho}{\pi \mu f}} \qquad \frac{\rho}{\delta \omega} = \frac{1}{2}\sqrt{\frac{\mu \rho}{\pi f}} \quad .$$

Therefore we can express the ratio Q_e to Q_u as

$$\frac{Q_e}{Q_u} = A\sqrt{\mu} + B \quad . \tag{24}$$

Experimentally a quantity p, which is proportional to reflected power, is measured.

$$p = cP_r = c|\Gamma|^2 P_i \quad . \tag{25}$$

This equation assumes that the amplifier used is linear. Therefore

$$\Gamma = \frac{p^{\frac{1}{2}}}{\alpha} \quad ,$$

where

$$\alpha = \sqrt{cP_i} \quad .$$

α may be determined by measuring the standing wave ratio ρ at one value of p. For the undercoupled case

$$\rho = \frac{1 + |\Gamma|}{1 - |\Gamma|} \quad . \tag{26}$$

In the case of an overcoupled cavity ρ is the same as above.

$$|\Gamma| = \frac{\rho - 1}{\rho + 1} \quad . \tag{27}$$

Then

$$\alpha = p^{\frac{1}{2}}\left(\frac{\rho + 1}{\rho - 1}\right) \quad . \tag{28}$$

Hence

$$A\sqrt{\mu} + B = \rho = \frac{1 + |\Gamma|}{1 - |\Gamma|} , \qquad (29)$$

$$= \frac{1 + p^{\frac{1}{2}}/\alpha}{1 - p^{\frac{1}{2}}/\alpha} , \qquad (30)$$

$$\doteq \frac{\alpha + p^{\frac{1}{2}}}{\alpha - p^{\frac{1}{2}}} , \qquad (31)$$

where A and B involve Q_c and Q_u and are constants for a given cavity at a given temperature. Thus, a quantity proportional to the effective permeability can be obtained from measurments made on the cavity.

III. EXPERIMENTAL APPARATUS AND PROCEDURE

A. MICROWAVE APPARATUS

The apparatus is the conventional microwave apparatus as shown in the block diagram (Figure 4). The klystron is a 723AB low power oscillator operating at about 9000 megacycles per second. It is modulated with a 1000 cycles per second square wave which, along with necessary DC voltages, is isolated from the load by a flap attenuator. The klystron and attenuator are matched with a Hewlett-Packard E-H tuner to the H-arm of a magic T. The E-arm is matched with another E-H tuner. The output of the matched detector is read on a Browning TAA-16 twin-tee tuned amplifier peaked to match the frequency of the square wave. The two side arm of the T feed the energy to a matched load coupled to one arm and through a standing wave detector to the resonant cavity, coupled to the other arm. Energy from the klystron is coupled into the two side arms but not into the E-arm of the T. That portion of the energy which goes into the arm with the matched load is completely absorbed. The portion which goes in to the arm with the cavity is reflected from the cavity and partially coupled into the E-arm. Only power that is reflected from the cavity goes into the E-arm. This is the power that is measured by the detector, and the meter reading is proportional to this reflected power. The matching devices prevent any multiple reflections in any of the arms of the T. The overall matching of the system is to a volt-

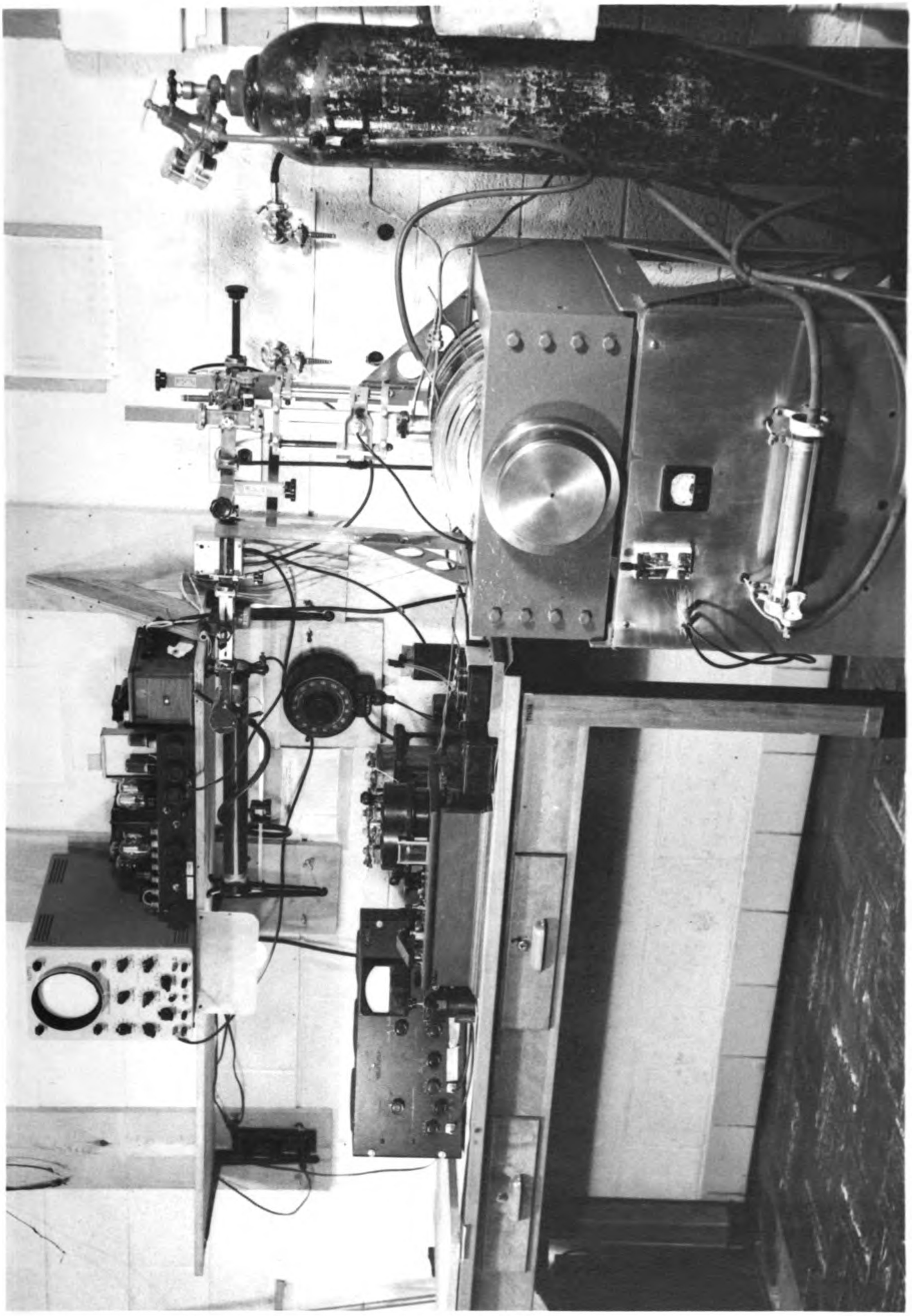

FIGURE 3 APPARATUS

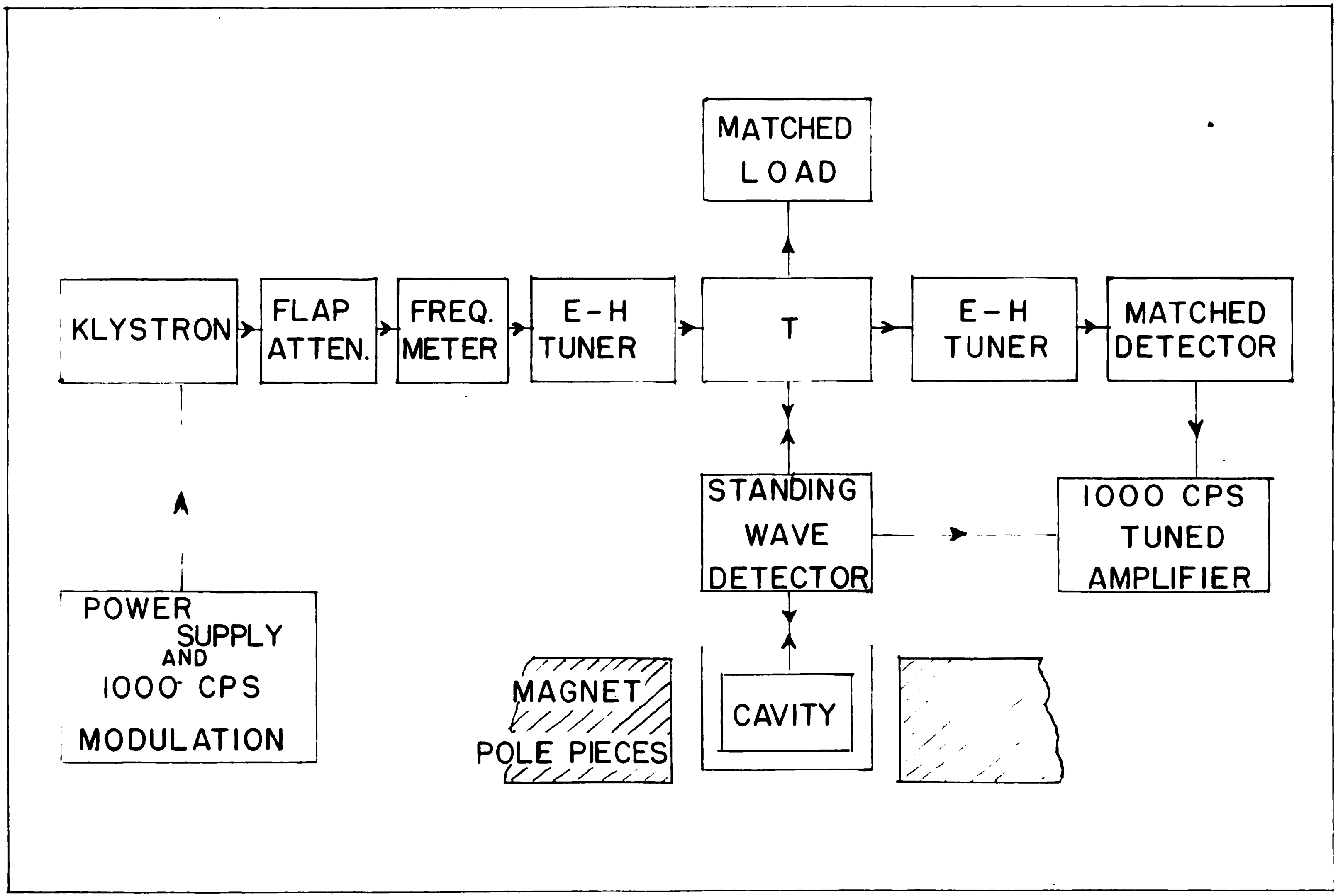

FIGURE 4 BLOCK DIAGRAM OF APPARATUS

age standing wave ratio of about 1.05 except in the arm containing the resonant cavity. In this arm, the standing wave ratio is determined by the type of cavity used. A mica window was cemented in the guide to prevent leakage of the hydrogen gas which was used as a reducing atmosphere. The mica introduced so little reflection that it was not necessary to match these reflections out.

The resonant cavity used was three half wave lengths long. It was coupled to the guide with a symmetrically placed circular iris. An iris with a diameter less than 5/16 inch resulted in an undercoupled cavity. An undercoupled cavity was used throughout the experiment. The cavity was assembled with silver solder. Silver solder was used because of its high melting point. Oxidation was removed from inside the guide by polishing with a fine grade of carborundum and then washed with a 10% solution of nitric acid.

The sample was plated on a brass disks (copper disks were also used). The disk was then silver soldered on the end of the cavity, thus completing the cavity. The preparation of the sample will be discussed later.

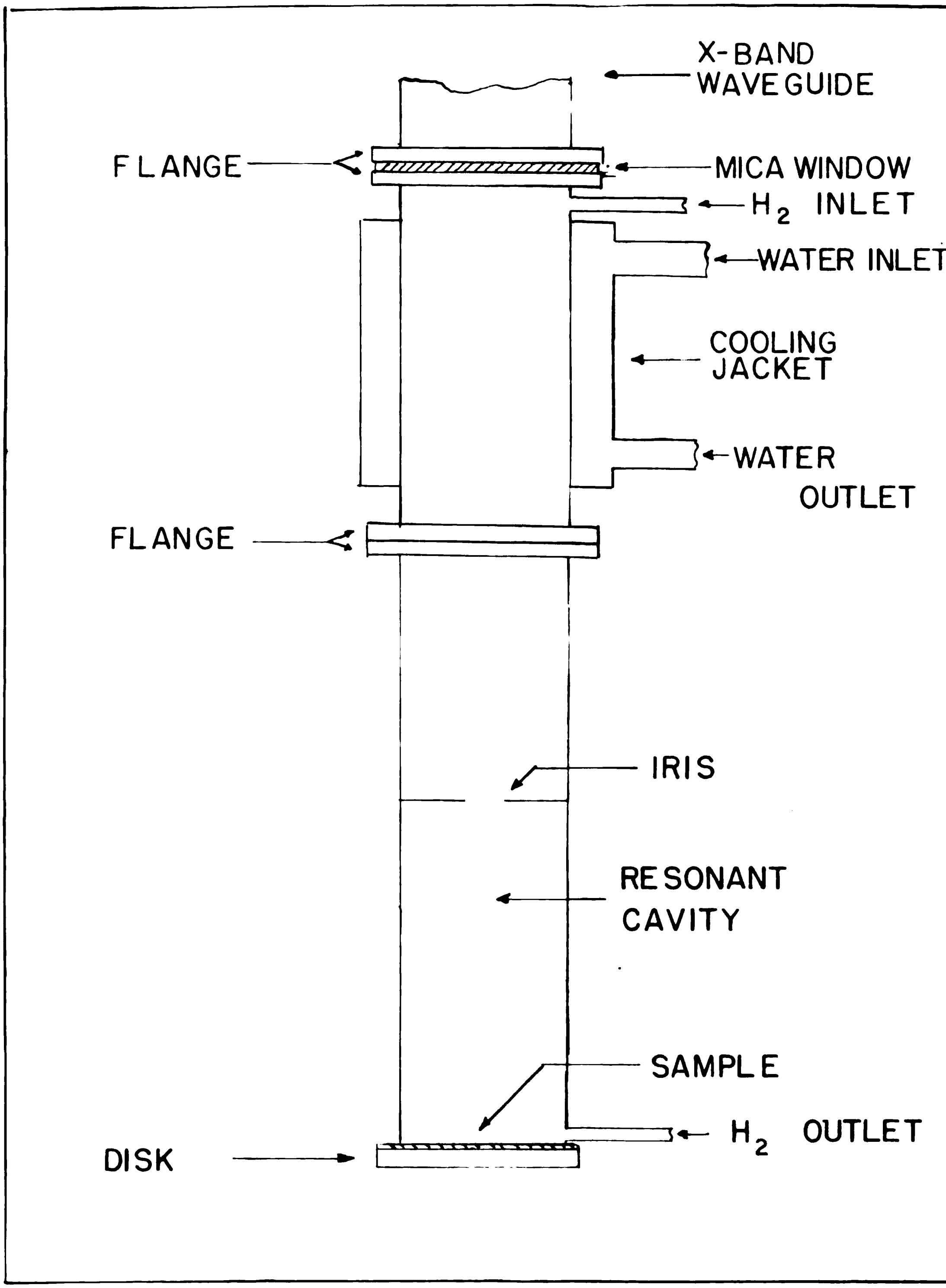

FIGURE 5 CAVITY ASSEMBLY

B. HEATING THE SAMPLE

The heating coil had resistance of approximately 9 ohms and was fabricated of .112 inch by .005 inch Nichrome ribbon wound on the cavity in a non-inductive manner. The coil was operated on AC supplied by a Variac. The coil was wound on a layer of asbestos on the cavity and was held in place by a layer of baked potters clay. An insulating layer of glass wool was wrapped on the clay. This oven was capable of temperatures up to 800 degrees centigrade with a power input of 500 watts. The temperature was measured with a calibrated Chromel-Alumel thermocouple inserted in disk on which the sample was plated. Thus making it possible to read the temperature at a point adjacent to the sample. The thermocouple was checked by Cowen[5] and was found to be accurate to 2 degrees centigrade from room temperature up through the range needed. The output of the thermocouple was read on a Leeds and Northrup type K potentiometer. The hydrogen gas in the cavity prevented oxidation of the sample at high temperatures. The gas entered above the cavity and passed out the bottom where it was burned. A water cooled section of the guide was placed above the cavity to prevent excessive heating of the rest of the microwave apparatus.

C. MAGNET

The magnet was constructed on SAE 1020 low carbon steel in the form of a square box 22 inches by 22 inches by 9 inches. The sides of the box which are 3½ inches thick were machined and bolted together with ½ inch bolts. The pole pieces are 7 inches in diameter. They were machined to slip fit holes bored in the box, and were threaded and held in place with retaining rings 1 inch thick. Because the ferromagnetic resonance line is very wide no special treatment of pole faces to insure a homogeneous field was undertaken. The copper wire used in the winding was .072 inches square formvar insulated wire which was wound on four copper bobbins. The bobbins were made of 3/16 inch thick copper sheet and were designed so that the finished spool was 15 inches in diameter and 1 3/4 inches thick. Each coil had a resistance of approximately 5 ohms. The wire was insulated from the bobbin with a layer of .010 inch asbestos paper. After winding, the coils were dipped in formvar and wrapped in linen. The two coils on each pole were connected in series. The windings on one pole were connected on parallel with those on the other pole. The magnet was cooled with 6 water coils made of ½ inch square copper tubing. It was found that the magnet itself did not heat up to any great extent. However, the cooling was necessary because of the high temperature to which the cavity was heated. The power source was a bank of 12 marine batteries with a 300 ampere hour capacity. The magnet was controlled with a water cooled rheostat. The current was read on a Westinghouse Type PX-4 ammeter to an accuracy of approximately 25 milliamperes in the range 0-5 amperes. Since the hysterysis of the magnet is approximately 65 gauss, care was taken in always taking readings with increasing current. The magnet was calibrated with a Sensitive Research Company model F. M. fluxmeter.

D. PREPARATION OF SAMPLE

The cobalt was plated on brass and copper disks. The disks measured 1 1/4 inches in diameter by 1/8 inch thick. The disks were polished with various grades of emery paper. The final polish was done with jewelers rouge until a near mirror finish was obtained. After polishing, the disks were thoroughly cleaned, first by washing with a detergent and then electrolytically in a special cleaning solution. The cleaning solution consisted of 23 grams of sodium carbonate, 23 grams of sodium triphosphate, 15 grams of sodium hydroxide, and 8 grams sodium meta silicate dissolved in one liter of water. The sample to be cleaned was used as cathode. The current density used was of the order of 5 amperes per square inch. The disks were then plated in a solution containing cobalt sulphate, magnesium sulphate and ammonium sulphate. The current density used was .012 amperes per square inch. Oxidation at room temperature was unimportant with cobalt plates. For this reason it was possible to plate several

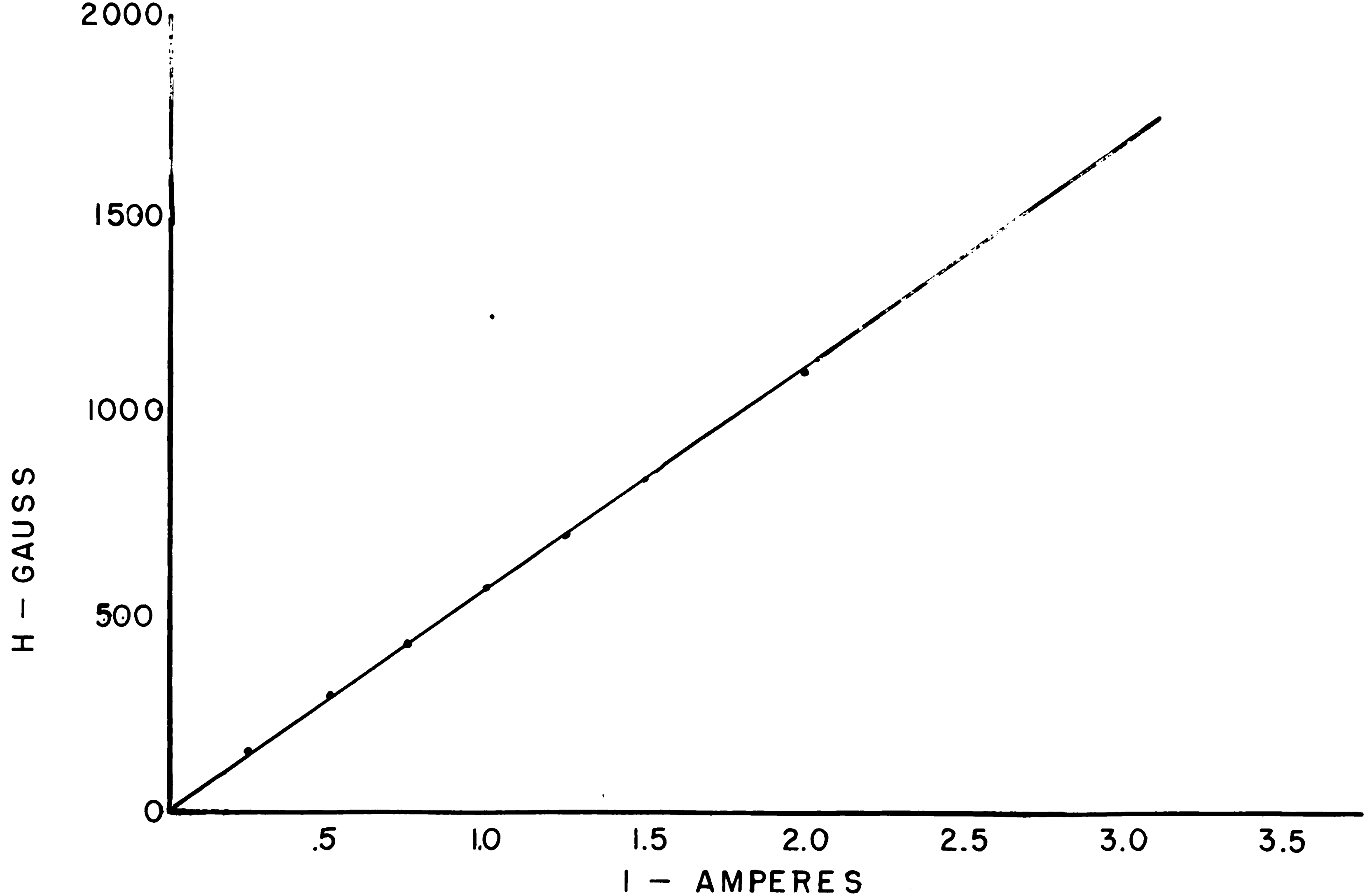

FIGURE 6 MAGNET CALIBRATION

samples at one time and then store them. It was not necessary to polish the sample after plating. A bright plate was relatively easy to obtain. The samples were then ready to be silver soldered to the guide to form the resonant cavity. Hydrogen gas was used as a reducing atmosphere in the soldering process.

IV. REDUCTION OF DATA

It is desirable to construct a quantity which depends on μ but does not involve the unknown constants of equation (31), namely A and B. By so doing we can eliminate the evaluation of these constants. Rewriting equation (31)

$$A\sqrt{\mu} + B = \frac{a + p^{\frac{1}{2}}}{a - p^{\frac{1}{2}}} . \tag{31}$$

Let μ_{res} be the value of μ at ferromagnetic resonance. Equation (31) becomes

$$A\sqrt{\mu_{res}} + B = \frac{a + p_{res}^{\frac{1}{2}}}{a - p_{res}^{\frac{1}{2}}} . \tag{32}$$

At very large values of H_0, μ should equal unity. Hence

$$A + B = \frac{a + p_{\infty}^{\frac{1}{2}}}{a - p_{\infty}^{\frac{1}{2}}} . \tag{33}$$

Combining equations (31), (32), and (33) we get,

$$R = \frac{\sqrt{\mu} - 1}{\sqrt{\mu_{res}} - 1} = \left(\frac{p^{\frac{1}{2}} - p_{\infty}^{\frac{1}{2}}}{p_{res}^{\frac{1}{2}} - p_{\infty}^{\frac{1}{2}}}\right)\left(\frac{a - p_{res}^{\frac{1}{2}}}{a - p^{\frac{1}{2}}}\right) . \tag{34}$$

R involves only equantities which can be measured directly. It can easily be determined as a function of H_0. Next it must be shown that $1/T_2$ can be found from R (H_0). The method employed to find $1/T_2$ is approximate. The exact method is considerable more tedious. Although the method is approximate its accuracy may well be within the limits imposed by the fundamental data.

Let $H_{0\frac{1}{2}}$ and $H_{0\frac{1}{2}}$ be two values of H_0 such that

$$\omega_0^2 - \omega^2 = \frac{2\omega}{T_2} \; ; \qquad H_0 = H^+_{0\frac{1}{2}} \tag{35}$$

$$\omega_0^2 - \omega^2 = -\frac{2\omega}{T_2} \; ; \qquad H_0 = H^-_{0\frac{1}{2}} \quad . \tag{36}$$

From equations (8) it can be seen that $H^+_{0\frac{1}{2}}$ and $H^-_{0\frac{1}{2}}$ are solutions of

$$H^2_{0\frac{1}{2}} - H^2_{o\,res} + 2\eta(H_{0\frac{1}{2}} - H_{o\,res}) \pm \epsilon = 0 \quad , \tag{37}$$

where

$$2\eta = (N'_x + N'_y - 2N'_z)M_0 \quad , \tag{38}$$

and

$$\epsilon = \frac{2\omega}{\gamma^2 T_2} \quad .$$

Then

$$H^+_{0\frac{1}{2}} + \eta = \left[(H_{o\,res} + \eta)^2 + \epsilon\right]^{\frac{1}{2}} \quad , \tag{39}$$

and

$$H^-_{0\frac{1}{2}} + \eta = \left[(H_{o\,res} + \eta)^2 - \epsilon\right]^{\frac{1}{2}} \quad . \tag{40}$$

We define the line width as

$$\Delta H \equiv H^+_{0\frac{1}{2}} - H^-_{0\frac{1}{2}} \quad . \tag{41}$$

Expanding the right side of equations (39) and (40) by the binomial theorem,

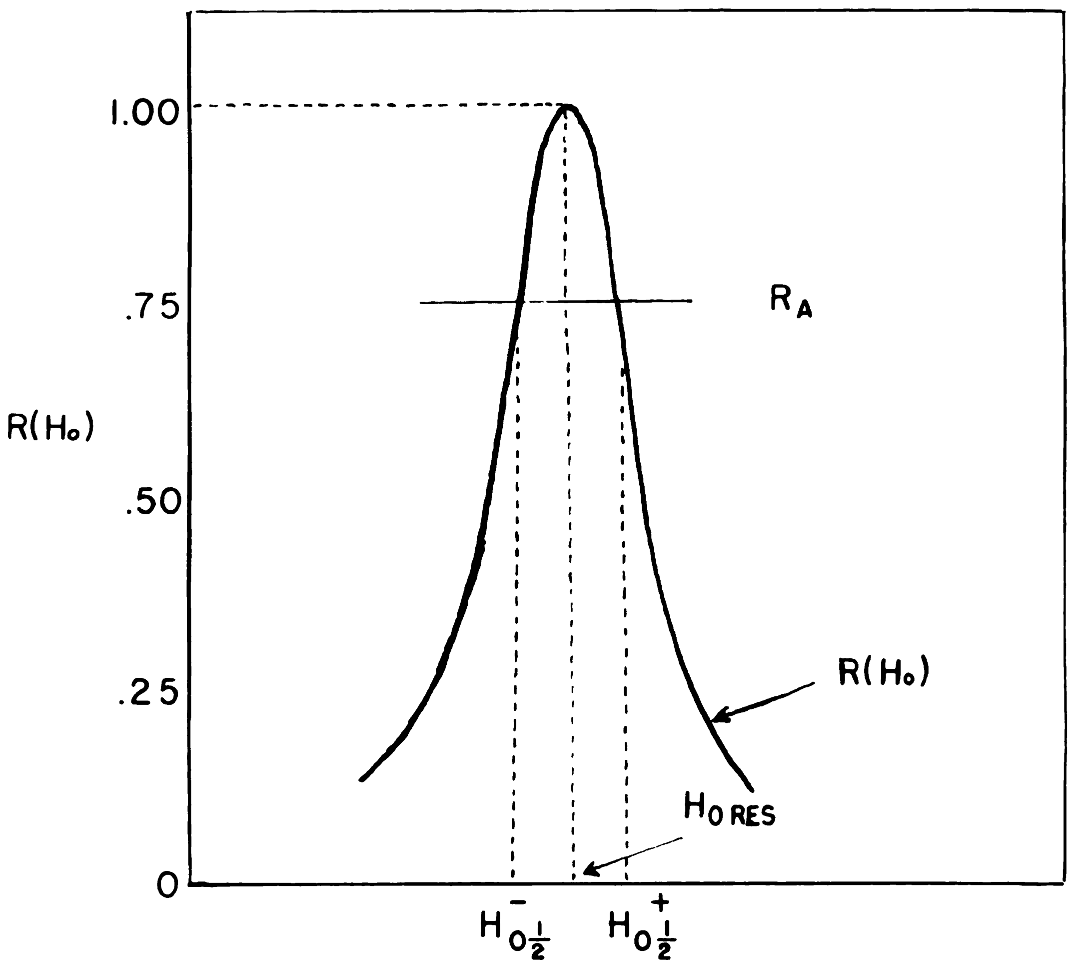

FIGURE 7 THE METHOD OF DETERMINING H_o^+ AND H_o^- FROM THE EXPERIMENTAL CURVE R(H)

$$\Delta H = \frac{\epsilon}{H_{o\,res} + \eta}\left[1 + \frac{1}{8}\left(\frac{\epsilon}{H_{o\,res} + \eta}\right)^2 + \cdots\right] . \qquad (42)$$

Upon examination it can be seen that the second term will be small compared to the first term and therefore may be dropped.

Then

$$\epsilon \cong \left(H_{o\,res} + \eta\right)\Delta H \quad , \qquad (43)$$

and

$$\frac{1}{T_2} \cong \frac{\gamma^2}{2\omega}\left(H_{o\,res} + \eta\right)\Delta H \quad . \qquad (44)$$

Thus by measuring the resonance field and the line width we can evaluate $1/T_2$. ΔH can be obtained from a plot of R (H_0). Let $\mu^{+}_{2\frac{1}{2}}$ and $\mu^{-}_{2\frac{1}{2}}$ be the values of μ_2 at H_0 equal to $H_{0\frac{1}{2}}$ and $H_{0\frac{1}{2}}$ respectively. From equations (7), (35), (36)

$$\mu^{+}_{2\frac{1}{2}} \cong \mu^{-}_{2\frac{1}{2}} \cong \frac{1}{2}\mu_{2\,res} \quad . \qquad (45)$$

The superscripts and will now be dropped. From (6),

$$\mu_{1\frac{1}{2}} \cong \mu_{2\frac{1}{2}} \cong \frac{1}{2}\mu_{2\,res} + 1 \quad . \qquad (46)$$

From the expressions

$$\mu' = (\mu_1^2 + \mu_2^2)^{\frac{1}{2}} + \mu_2 \quad ,$$

and from (45), and (46)

$$\mu'_{\frac{1}{2}} \cong \left[(1 + \tfrac{1}{2}\mu_{2\,res})^2 + (\tfrac{1}{2}\mu_{2\,res})^2\right] + \tfrac{1}{2}\mu_{2\,res} \quad . \tag{47}$$

Similarly,

$$\mu'_{res} \cong \left[1 + (\mu_{2\,res})^2\right]^{\frac{1}{2}} + \mu_{2\,res} \quad . \tag{48}$$

These expressions for $\mu'_{\frac{1}{2}}$ and μ'_{res} are inserted in equation (34) giving the ratio,

$$R_a = \frac{\left\{\left[(1 + \frac{1}{2}\mu_{2\,res})^2 + (\frac{1}{2}\mu_{2\,res})^2\right]^{\frac{1}{2}} + \frac{1}{2}\mu_{2\,res}\right\}^{\frac{1}{2}} - 1}{\left\{\left[1 + (\mu_{2\,res})^2\right]^{\frac{1}{2}} + \mu_{2\,res}\right\}^{\frac{1}{2}} - 1} \quad . \tag{49}$$

The intersections of R_a with R (H_0) give approximate values of $H^+_{0\frac{1}{2}}$ and $H^-_{0\frac{1}{2}}$. R_a varies slowly with $\mu_{2\,res}$ as shown by Table I.

TABLE I

VALUES OF R_a FOR VARIOUS VALUES OF $\mu_{2\,res}$

$\mu_{2\,res}$	R_a
65	.759
60	.758
55	.757
50	.757
45	.756
40	.755
35	.754
30	.753
25	.751

An approximate method is now needed for calculating $\mu_{2\,res}$. From equations (7) and (44),

$$\mu_{2\,res} \cong \frac{4\pi M_0(H_{o\,res} + 4\pi M_0)}{\Delta H(H_{o\,res} + \eta)} \tag{50}$$

We find $1/T_2$ by proceeding as follows:

1. Data consists of a plot of p against applied field H_0. ρ is measured at a point near resonance. α can be calculated from equation (28). $R(H_o)$ can be obtained from equation (34).

2. Assume $R_a \approx .75$. Draw a line on the plot of $R(H_o)$ at .75 and read off the distance between intersection points. This the first approximation of ΔH .

3. From equation (50) calculate $\mu_{2\,res}$. Find the corresponding value of R_a from Table I. Then from the plot of $R(H_o)$ find second approximation of ΔH.

4. Calculate $1/T_2$ from equation (44).

Usually two approximations are sufficient to give all the available accuracy in this method. The advantage of using the above method is eliminating the necessity of evaluating the constants A and B of equation (31). These constants involve the uncertain conductivities of the cavity walls. If they are introduced they increase the possibility of erroneous results.

Values of the demagnetization factors and the saturation magnetization had to be inserted in reducing the data. The total demagnetization factors consist of the sum of the shape demagnetization factors and the anisotropy factors.

$$N_x' = N_x + N_x^a \quad .$$
$$N_y' = N_y + N_y^a \quad . \qquad (51)$$
$$N_z' = N_z \quad .$$

The N^a's are anisotropy factors and the N's are shape demagnetization factors. Since the sample used in this experiment is isotropic, the anisotropy terms can be dropped. The shape demagnetization factors for thin oblate spheroids are,

$$N_x = \frac{\pi^2}{m}\left(1 - \frac{4}{m\pi}\right)$$
$$N_y = 4\pi\left(1 - \frac{\pi}{2m} + \frac{2}{m^2}\right) \qquad (52)$$
$$N_z = \frac{\pi^2}{m}\left(1 - \frac{4}{m\pi}\right) \quad ,$$

where m the ratio of the diameter to the thickness. The appropriate thickness for N_z is the actual thickness of the spheroid, because H_o is oriented along z. The x and y components of the magnetic field are r-f components and therefore the effective thickness of the spheroids for N_x and N_y is the skin depth. Therefore for thin spheroids,

$$N_x \cong 0$$
$$N_y \cong 4\pi \qquad (53)$$
$$N_z \cong \frac{\pi^2}{m} \quad .$$

V. RESULTS

Figure 8 shows a typical resonance curve for electroplated cobalt. There is only one resonance peak on the curve. Through the range of temperature possible with the apparatus, there was no apparent change in this resonance peak, which came at about 440 gauss.

It was not possible to reach the Curie temperature for cobalt, which is 1120 degrees centigrade, with the available apparatus. The highest temperature reached was about 700 degrees centigrade. At this point the apparatus broke down on each trial. This temperature appeared to be the limit of the heater coil. Also at temperatures above 700 degrees centigrade the silver solder melted and gave away to the pressure of the hydrogen gas in the cavity, and with a hole in the cavity, the microwave resonance dissappeared.

Figure 9 represents data on $1/T_2$ as a function of temperature for electroplated cobalt. In the range of temperatures in which measurements of $1/T_2$ were made, $1/T_2$ tended to reach a nearly constant value of 17×10^9 second^{-1} as the temperature increased. All of the samples used gave different values of $1/T_2$ for room temperature, but tended to flatten at approximately the same value for $1/T_2$.

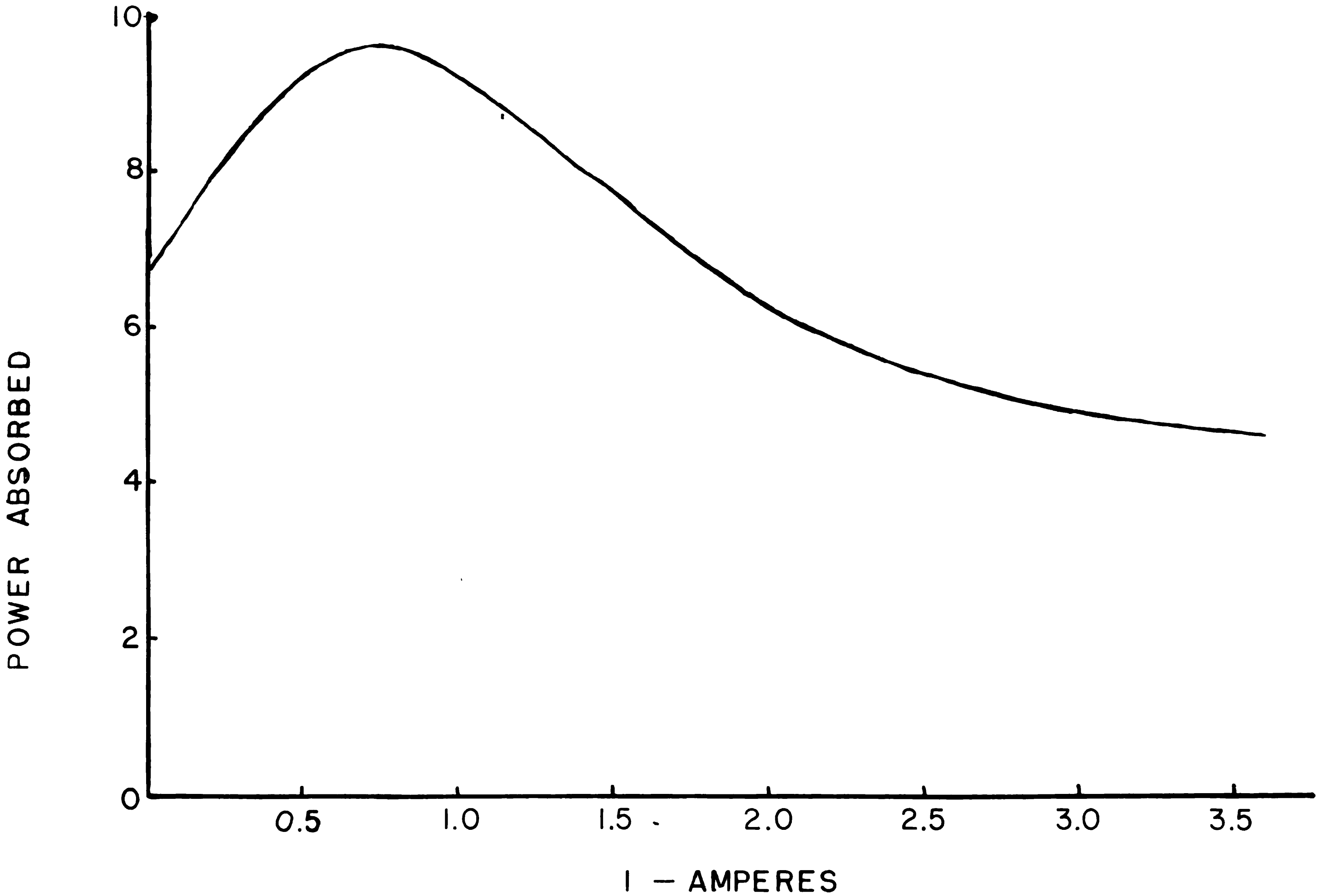

FIGURE 8 TYPICAL RESONANCE CURVE FOR ELECTROPLATED COBALT

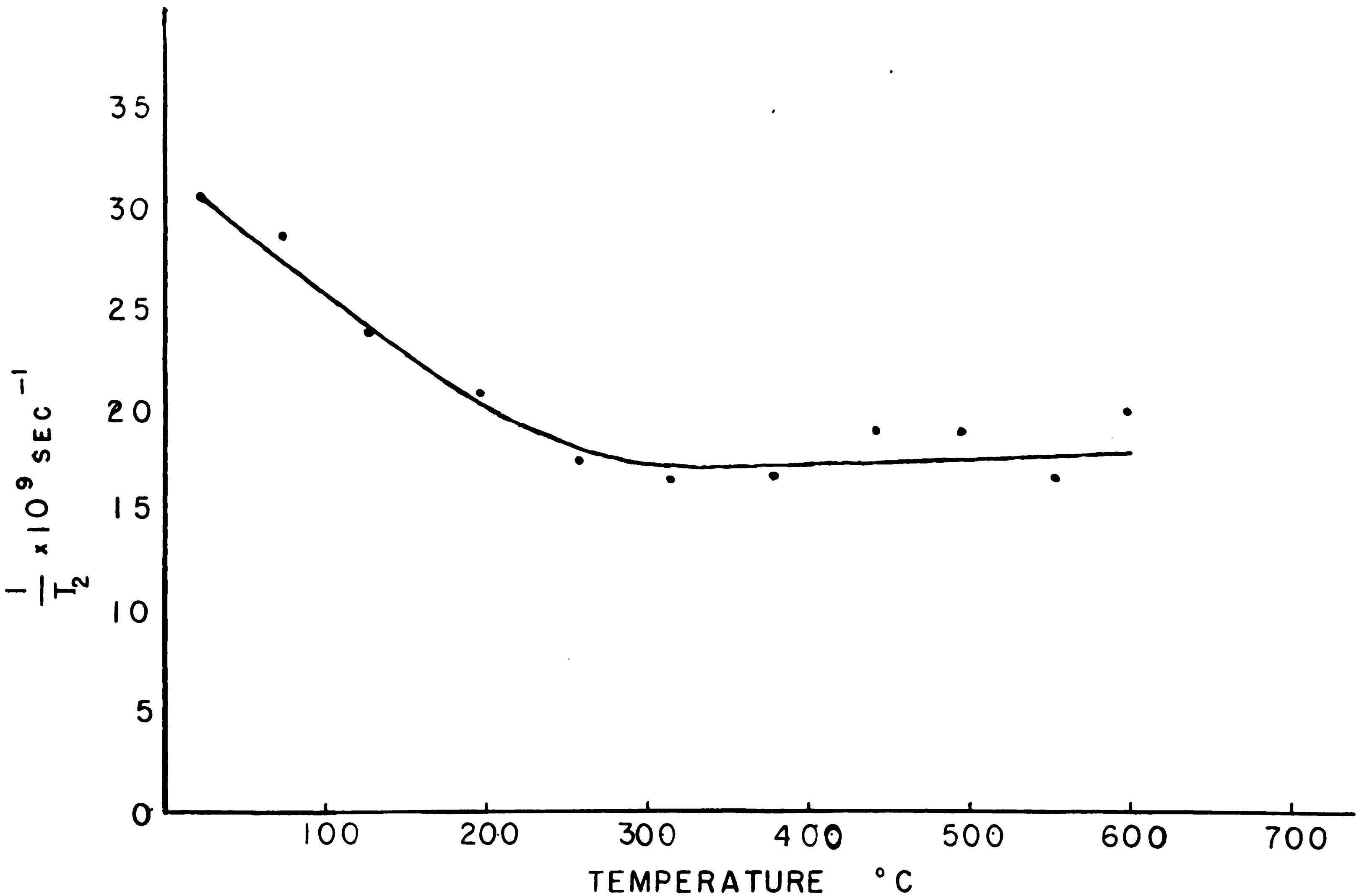

FIGURE 9 TEMPERATURE DEPENDENCE OF $\frac{1}{T_2}$ FOR ELECTROPLATED COBALT

APPENDIX

ANISOTROPY ENERGY IN ELECTROPLATED COBALT

In this experiment the ferromagnetic material used were cobalt. The cobalt was used in an electroplated form. An electroplated material is generally assumed to be polycrystalline, that is, there is every possible crientation of the crystals of the material.

In an uniaxial crystal, such as cobalt, the anisotropy energy is,

$$E_k = K_0 + K_1 \sin^2\theta + K_2 \sin^4\theta \ , \tag{1}$$

where K_0, K_1 and K_2 are the crystal anisotropy constants, and θ is the angle between the magnetization vector and the principal axis of the crystal. To find the anisotropy energy in a polycrystalline material it is necessary to find the average of E_k in all directions,

$$\iint E_k \, d\Omega = \langle E_k \rangle_{ave} \tag{2}$$

After substituting

$$\int_0^{2\pi}\int_0^{\pi}(K_0 + K_1\sin^2\theta + K_2\sin^4\theta)\sin\theta' d\theta' d\theta = \langle E_k \rangle_{ave} \ . \tag{3}$$

The coordinate axes can be picked such that $\theta = \theta'$

Hence

$$\left\langle E_k \right\rangle_{ave} = 0 \tag{4}$$

Therefore the average anisotropy energy in electroplated cobalt is zero.

BIBLIOGRAPHY

1. J. H. E. Griffiths, Nature 158, 670 (1946)
2. A. F. Kip and R. D. Arnold, Phys. Rev. 75, 1556 (1949)
3. N. Bloembergen, Phys. Rev. 78, 572 (1950)
4. D. W. Healy Jr., Phys. Rev. 86, 1009 (1952)
5. R. D. Spence and J. A. Cowen, O. O. R. Report (1954)
6. J. A. Cowen, Ph.D. Thesis, Michigan State College (1954)
7. C. Kittel and E. Abrahams, Rev. of Mod. Phy. 25 233 (1953)
8. C. Kittel and E. Abrahams, Phys. Rev. 90, 238 (1953)
9. C. Kittel and C. Herring, Phys. Rev. 77, 725 (1950)